

## **Sediment Dynamics Of Tropical Open Coast Beaches, Central West Coast Of India - Implications Of Spatio-Temporal Variability**

**Lynda-Uta Edet Okon<sup>1,2,4\*</sup>, Jaya Kumar Seelam<sup>2,3</sup>, Suneeta Kumari<sup>2</sup> and Lavanya Hemanath<sup>2</sup>**

**L.E.O.:** [ORCID® 0000-0002-7252-4220](https://orcid.org/0000-0002-7252-4220)

**J.K.S.:** [ORCID® 0000-0003-0406-3204](https://orcid.org/0000-0003-0406-3204)

**S.K.:** [ORCID® 0000-0001-9046-405X](https://orcid.org/0000-0001-9046-405X)

**L.H.:** [ORCID® 0000-0003-1387-7576](https://orcid.org/0000-0003-1387-7576)

<sup>1</sup> Bharathidasan University, Tiruchirappalli, Tamil Nadu, India

<sup>2</sup> CSIR-National Institute of Oceanography, Dona Paula, Goa, India

<sup>3</sup> Academy of Scientific and Innovative Research, School of Oceanography, Goa, India

<sup>4</sup> Institute of Oceanography, University of Calabar, Calabar, Nigeria

\* Corresponding author email: lyndaokon@gmail.com

### **Abstract**

Local and regional climatic pressures influence coastal geomorphic systems on different spatial and temporal scales. Within these zones of variation, systems and environmental processes interact. They can recreate sediment movement patterns and anticipate environmental evolution. This study utilises a non-parametric end-member modelling analysis (EMMA) as a deterministic approach for unmixing grain sizes into geologically relevant populations. The aim is to characterise seasonal grain size distribution variation and link seasonal end members to proximal sources. A five-year analysis of seasonal data from 19 open-coast beaches is adopted in the North and South Goa coastal area. End-members (EMs) are assigned based on grain size modal classes of 32 – 63 µm (EM1), 63 – 125 µm (EM2), 125 – 250 µm (EM3), and 250 – 500 µm (EM4), corresponding to coarse silt, very fine sand, fine sand, and, medium sand respectively. In response to the current hydrodynamic forcings, it is projected that the surface sediments analysed have been reworked, sorted, and redistributed. While the spatial trend of EM distribution indicates an abundance of EM2 and EM3 along the coast, the variability in EMs across seasons shows that the Southwest and Northeast monsoons significantly influence the distributions of sediments along the Goa coast, and the underlying EMs in the sediments bear the imprint of the interaction of these two seasons' dominant forces.

**Keywords:** Grain size, beaches, climate, EMMA, Spatio-temporal variability

## 1. Introduction

A thorough understanding of coastal sediments' intrinsic properties, provenance, and transport history is crucial due to the complexities of energy transfer in fundamental coastal processes (Blott and Pye 2001; Goudie 1991; Merkus 2009; Ramsey 1999). Examining the present geographical and temporal fluctuation of sediment characteristics within the context of known environmental factors (climate, tectonics, and human activities) is a requirement for extracting signals from sediments and reconstructing signal-related process parameters from the past (Diekmann and Kuhn 1999; McLaren et al. 2007; Orpin and Woolfe 1999). Sediment sorting involves the mechanical deterioration of grains and dynamic entrainment, transport, or deposition of grains with defined sizes, shapes, and densities and can be modelled as continuous fractionation processes (Le Roux and Rojas 2007). In earlier studies, sediments were statistically classed using parameter terms like median, mean, sorting, skewness, and kurtosis (Folk and Ward 1957; Friedman 1967; Passega 1964; Poizot et al. 2008; Sahu 1964). Despite their probabilistic nature, these parameters' spatial patterns exhibit predictable tendencies that reveal their dependence on a particular set of energy circumstances as a function of time and location (Alharbi et al., 2016; Fitch et al., 2015; Parthasarathy et al., 2016; Titocan et al. 2018). Consequently, they have been used to deduce patterns in fluvio-marine interactions in coastal locations (Angusamy and Rajamanickam 2006; Bhat et al. 2002; Trivedi et al. 2012). However, the variations in grain size statistical measures cannot fully represent sediment transport and deposition without considering the dynamic environment (Dietze et al., 2012; Hartmann, 2007).

Within a sedimentary environment, diverse sediments formed inside a sediment sink indicate sedimentation's primary driving forces and orientations. In order to analyse these process-related data, individual archive characteristics are insufficient, necessitating the separation of linked attributes. As a result, controlling the uncertainty associated with concepts, methods, and scales is necessary, which might result in random fluctuations (Hartmann 2007). One of the quantifiable attributes is sediment particle size, which characterises sediment qualities and the processes connected with them (*i.e.*, geomorphological, sedimentological, hydrological).

End-Member Modelling Analysis (EMMA) analysis is an essential tool in sedimentology for detecting subpopulations within sediment grain size distributions (GSDs) that are not readily apparent in individual sample GSDs. End-members (EM) are sediment grain size classes associated with various origins and transport mechanisms (Weltje and Prins 2007; Yu et al. 2016). Therefore, this method is widely employed to discretise their entrainment to learn more about selected sediments' origin, sedimentary environment, and climatic conditions (Dietze et al., 2013; Prins et al., 2002, 2007; Prins and Weltje, 1999). A few examples of end-member modelling approaches for

unmixing GSDs include EMMA (Weltje 1997), *AnalySize* (Paterson and Heslop 2015), BEMMA (Yu et al. 2016), and DRS-unmixer (Heslop et al. 2007). This method has been employed in provenance analysis (Prins et al. 2000; Shang et al. 2016), evaluating monsoonal influence (Dietze et al., 2013; Hamann et al., 2008), and estimating the effects of near-bottom currents, turbidity flow, and storm floods (Dietze et al. 2014; Dietze et al. 2013; Hamann et al. 2008; Van Der Lubbe et al. 2015; Zhang et al. 2013).

The Goa coast, a 130-kilometre-long coastal plain that runs between the Western Ghats and the Arabian Sea, is the northernmost extension of the Western Coastal Plains of India (Kunte et al. 2014a; Nadaf, 2019). It is divided into fundamental morphological units, including a vast stretch of lowlands adjacent to the coastal plain, low dissected denudational hills and tablelands to the east, and severely dissected high Western Ghats denudational hills that span the district's easternmost half (Kunte et al. 2014a). The rocks below define the drainage system with a characteristic dendritic pattern (Central Ground Water Board (CGWB), 2013).

Geologically, Goa comprises Precambrian and Cuddapah rocks, Sahyadri high plateaus and the Dharwars (quartzites, meta-greywackes, and banded hematite quartzite (Wagle 1993). The Cuddapah period's non-fossiliferous meta-sediments are heavily intruded by basic dykes. The Deccan Traps in the northeast comprise an ancient crystalline formation. The Sahyadri high plateaus, which define the coastline, are predominantly made up of reddish-brown sand and lateritic soil of the Quaternary age (Wagle 1993; Wilson et al. 2014; Nadaf, 2019) and is marked by a notable sand-dune belt with mild slopes broken by crusts and troughs formed by wind and wave action (Aparna et al. 2005). Ahmed (1972) categorised the coastline of Goa as a "submerged rocky, indented shoreline." The geomorphic features of the coastline, including sandy beaches, rocky beaches, sea caves, estuaries, mangroves, bays, headlands, cliffs, hills, corals, ports, harbours, and coastlines, are indicative of the marine erosional and depositional processes that occur there (Nadaf 2019).

Oceanographic changes on the central west coast of India occur seasonally: the Southwest monsoon (SWM; June–September) and Northeast monsoon (NEM; October–January) monsoons and Pre-monsoon (PRM; February–May) (Kumar et al. 2006; Dwarakish et al. 2009; Anoop et al. 2015; Fernandes et al. 2018). Wind and wave patterns vary substantially by season, with a humid tropical environment marked by abundant rainfall (about 87%), high humidity, and massive river runoff during the southwest monsoon (Chempalayil et al. 2014). Zuari (ZR) and Mandovi (MDV) estuaries, as well as Baga, Chapora and Sal rivers, are vital drainage systems along the Goa coast with high monsoonal discharge (Shetye et al. 2007; Manoj et al. 2009; Kessarkar et al. 2010).

The wind blows in the southwest direction during the SWM, and the waves are swells with periods ranging from 8 to 10 seconds (Shanas & Sanil Kumar, 2014). The MDV and ZR rivers flow roughly around 20 m<sup>3</sup>/s in the NE monsoon, which is minuscule compared to the 400 m<sup>3</sup>/s discharge during the SWM (Niraj et al. 2015). Their neap and spring tide amplitudes range from 0.25 to 2.3 metres (Chandramohan et al. 1998; Sundar and Shetye 2005). River mouths complicate sediment interaction. As a result, there is a significant influx of terrigenous sediment to the coast via runoff from these rivers (Suprit and Shankar 2008). Shah et al. (2020) reported that river-derived clays dominate the nearshore areas (mean annual sedimentation rate of 0.26 cm) up to 30 m, 20 kilometres from the coast. Additionally, headland erosion (wave energy convergence) and offshore (sea transgression, particularly during storm waves and other episodic events such as cyclones) also constitute sediment sources along this coast (Loveson et al., 2014). Longshore currents along this coast alternate between NE and SW monsoons (Seelam et al. 2014). The SW, which is the more energetic, prevails over longshore sediment transport; hence, before and during the NE monsoon, longshore sediment movement trends southwards, but during the SW monsoon, it trends northward (Jayakumar et al. 2001).

Numerous aspects, such as seasonal fluctuations in beach profiles, longshore sediment transport, and hydrodynamics, have been meticulously investigated on the tropical beaches of India's central west coast (Jayakumar et al., 2001, 2002; Seelam et al., 2014; Wilson et al., 2014). According to reports, the significantly enlarged SWM is the driving force behind coastal dynamics in this region; hence the beaches along this coastline experience sediment dynamics as a result of locally generated and monsoon-generated wind waves (Amrutha et al., 2015; Anithamary et al., 2011; Chandramohan et al., 1992; Shetye et al., 2007). Wave refraction (Veerayya et al. 1981a), remote sensing, geomorphologic indicators (Kunte 1994; Dholakia et al. 1995; Orzech 1997; Jayakumar et al. 2001), numerical modelling (Prakash et al. 2021), and descriptive sedimentological techniques have all been used to study sediment transport along this coastline (Loveson et al., 2014; Veerayya, 1972; Veerayya & Varadachari, 1975; Wilson et al., 2014). Veerayya (1972) investigated the textural properties of sediments, changes in beach topography, and sediment transport and distribution along and across Calangute beach. Similarly, Veerayya & Varadachari (1975) explained sediment transport along the coast based on grain size data, environmental factors influencing beach deposits, and Calangute beach dune sediments. The investigation revealed the significance of the grain size criterion in the definition of beach zones. The observed variation in grain size features of the sediments (medium to coarse sands) can be related to the prevalent transport, erosion, and deposition processes in the studied area.

Veerayya et al. (1981a) conducted wave refraction measurements for waves striking Colva beach at various times. As a result of the influence of the major currents and the related circulation pattern in the surf zone, most of the sediments of Colva Beach were recirculated between the two promontories. Calangute and Colva beaches have also witnessed annual cyclical morphological changes (Veerayya et al., 1981b). These beaches reach their maximum sediment storage capacity during PRM, at which point the onset of the SWM winds and wave conditions produces a rapid pace of erosion, followed by a slower rate for the remainder of the monsoon season. Until August, when the beaches have the least amount of silt deposition, erosion occurs. Due to the wave climate, the beaches progressively recover during the NEM and winter months. These results are upheld in a similar study by Wilson et al. (2014). Kunte (1994) utilised topographic maps, aerial photographs, and Landsat images of the Goa coast to analyse the direction, size, and behaviour of longshore drift to distinguish between erodible and non-erodible coastal areas. According to his findings, accretion occurs throughout the NEM and PRM seasons, while deterioration occurs during the SWM season. In their examination of beach dynamics and coastal oscillations along Miramar beach, Loveson et al. (2014) also noticed a significant contribution from MDV derived from headland erosion of Cabo Raj and Aguada, offshore sources, and the hinterland.

Generally, these findings suggested a seasonal effect on beach morphology. However, while these previous studies have reported on bulk sediment distributions based on descriptive statistics from a few beaches along the Goa coastline and adjacent areas, the provenance of these sediments has not been well developed. These studies have also not considered the flow-substrate (fluid-sediment) interaction which defines the region's hydrodynamic controls on coastal sediment dynamics.

In this study, we incorporate EMMA into analysing the modern surface sediment dataset of the north and south Goa open coast beaches by examining the significance of the juxtaposition of regional climates on the heterogeneity of grain size distributions on the beach sediment along the Goa coast, central West of India over five years. We illustrate the spatial and seasonal signatures in sediment properties by decomposing reported GSDs into data-specific end members and categorising and interpreting them genetically using non-parametric goodness of fit methods in EMMA. The EMs are further evaluated for source assessment given proximal sources based on the average sediment grain size classes of the neighbouring rivers and nearshore areas. The validity of the EMMA results is assessed based on numerical and geological feasibilities. The study will provide index information to aid improved coastline management strategies.

## 2. Materials And Methods

This study covers the open coast beaches between Baga and Sinqerim in North Goa (NG) and Velsao to Mobor in South Goa (SG). In the region's transitional coastal-plain context, the sampling sites were chosen to achieve adequate geographic coverage and identify a broad selection of representative beaches (Fig 1; Table 1).

The NG coastline (Baga to Sinqerim) is steep and broad, with expansive dunes around it (Mascarenhas 1998a; Wilson et al. 2014b). Candolim's backshore is more developed, and its berm is greater than Calangute Beach's. Compared to Calangute's expansive coastline, Baga beach has a narrow backshore with a steep shoreline (Murty et al. 1982)

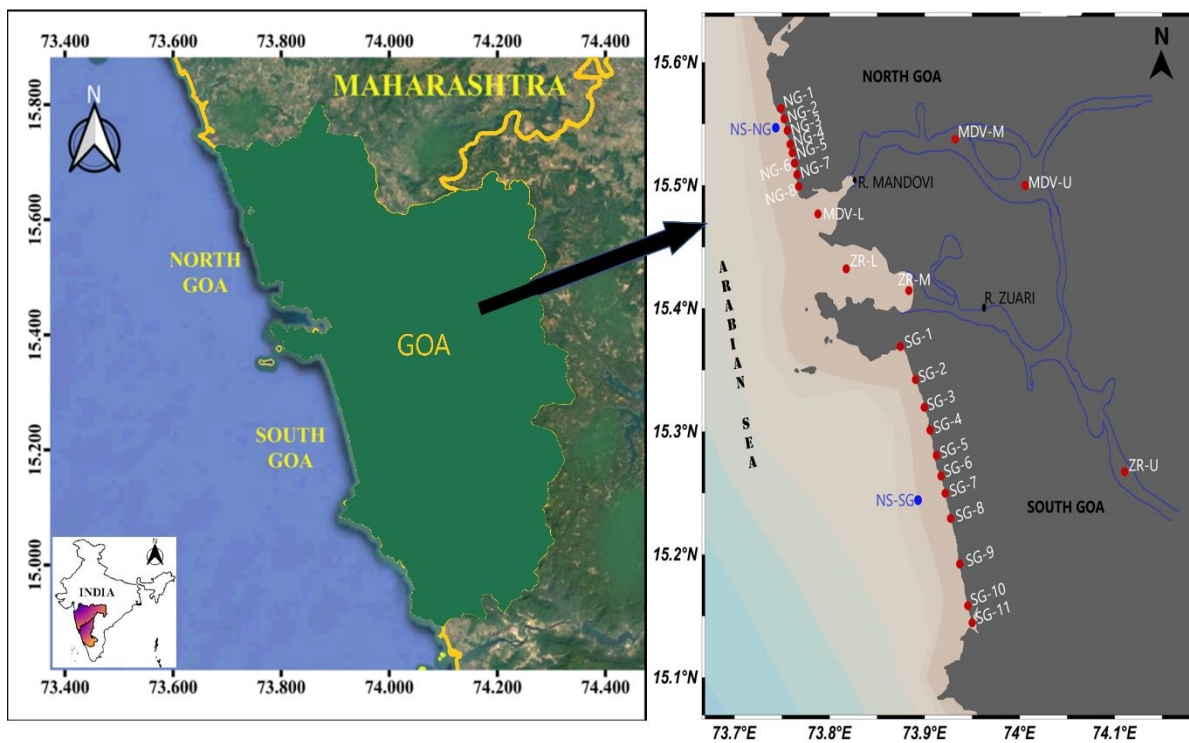


Fig 1

— Map showing the study region in Goa (left) and the study sites along the North Goa and South Goa coast (right). Right: Sampling stations for North Goa (NG 1 – 8); South Goa (SG 1 – 11); Nearshore North Goa (NS-NG, 10m water depth); Nearshore South Goa (NS-SG, 10m water depth); Mandovi Upper, Middle and Lower (MDV-U, MDV-M, MDV-L); Zuari Upper, Middle and Lower (ZR-U, ZR-M, ZR-L).

The SG beaches (Velsao to the Mobor Peninsula) are bounded to the north by the Zuari Estuary and to the south by the River Sal and are the most prominent and longest dunes belt along the coast. Velsao is home to modest dunes of sand. The Arossim - Mobor coastline zone contains vast 3-10 m high sand dunes with associated vegetation (Mascarenhas 1998). An annual hydrodynamic feature at Colva is an ephemeral beachfront lagoon. Degraded berms indicate that construction and sand

mining threaten most of the shoreline along this stretch. The NG and SG coastlines are renowned for water sports, amusements, and beach resorts, making a study on coastal and sediment dynamics beneficial for public safety.

Table 1 — Sampling stations for North Goa (NG 1 – 8); South Goa (SG 1 – 11)

NORTH GOA							
NG-1	NG-2	NG-3	NG-4	NG-5	NG-6	NG-7	NG-8
Baga 1 (Baga)	Baga 2 (Baga)	Calangute 1 (Cal)	Calangute 2 (Cal)	Candolim 1 (Cand)	Candolim 2 (Cand)	Sinquerium 1 (Sinq)	Sinquerium 2 (Sinq)
SOUTH GOA							
SG-1	SG-2	SG-3	SG-4	SG-5	SG-6	SG-7	SG-8
Velsao (Vel)	Arossim (Aro)	Majorda (Maj)	Betalbatim (Bet)	Colva (Col)	Benaulim (Ben)	Varca (Var)	Fatrade (Fatr)
SG-9	SG-10	SG-11					
Carmona (Car)	Cavellossim (Cav)	Mobor (Mob)					

## Hydrodynamics

A hindcast of ECMWF Reanalysis V5 (ERA5) data provides the Arabian Sea bulk wind fields and wave parameters (significant wave height ( $H_s$ ), wave period ( $T_p$ ), and mean wave direction). While ERA-Interim wind and wave data have considerable temporal variability, they perform well with measured counterparts (Glejin et al. 2013; Shanas and Sanil Kumar 2014a). This study estimated hourly averages of the bulk characteristics, using ERA5 data to characterise process-driven sediment distribution and correlate with regional climate and meteorology for three studied seasons across five years (2016-2020). For MDV and ZR rivers, river discharge rates were extracted from India Water Resources Information System (<https://indiawris.gov.in/wris/>).

## Sediment Sampling and Analysis

Surficial sediment sampling along the Goa coast beaches was conducted between 2016 and 2020 in April, July and November (except in April 2018 and Nov 2020). Samples were obtained during spring low tide at the beach face to support Bascom's (1951) concept of a zone of active sediment dynamics (i.e., sampling along the high tide line, mid-tide line, and low tide line). Two sets of nearshore samples (NS-NG and NS-SG; taken at 10m water depth) and six riverine (MDV-U, MDV-M, MDV-L, ZR-U, ZR-M, ZR-L) samples were obtained in April 2019 using a Van Veen grab sampler.

The beach sediment samples were homogenised and quartered to 100 g in the laboratory for sieve analysis. The samples were desalinated by repeatedly washing them in deionised water. The samples were then disaggregated with 10% hexametaphosphate, treated with 30% hydrogen peroxide to eliminate organic content, and dried at 65°C.

Intermittent sieving of beach samples was carried out using a mechanical sieve shaker for 15 minutes with seven ASTM sieves No. 10, 18, 35, 60, 120, 230, 450 with corresponding mesh sizes of 2mm, 1mm, 500µm, 250µm, 125µm, 62.5µm and 31.25µm. The results from this analysis were used as input bins for the end member modelling analysis. Even though the EMMA method requires as many grain-size classes as there are likely numerous end-members in a data set, it is essential to specify the end-member grain-size distributions by the number of grain-size classes that must be suitably recognised (Paterson and Heslop 2015).

Sediment samples obtained from the riverine and nearshore areas were predominantly mud. Hence, the standard analytical protocol for laser particle analysis following Konert & Vandenberghe (1997), using the Malvern Mastersizer 2000 (measurement range of 0.02–2000 µm), was adopted. These results were not subjected to EM analysis to avoid conflict in experimental procedures and were reported based on bulk descriptive statistics.

Bulk descriptive statistics for all analysed datasets were interpreted after Folk and Ward's (1957) geometric (modified) graphic measures (Blott and Pye 2001).

### **Algorithm for End Member Modelling Analysis (EMMA)**

End-member modelling allows investigations into the causes of grain size variability over time and space that are difficult to establish using univariate grain-size data alone (Dietze et al. 2012, 2013, 2014; Dietze and Dietze 2019). The analysis satisfies all requirements for non-negative and unit-sum distributions. The assessment of the geological viability of end members was performed by multi-statistical approaches and field data to highlight the inherent variability of end members. A succession of GSDs from the identical depositional sequences was used to identify the EM shape following Weltje and Prins (2007). To solve the mixing problem, non-parametric end member unmixing methods are applied thus:

$$Y = S \cdot C + E$$

Where  $S$  is a matrix containing GSD end members,  $C$  is the weighting of the end members in each sample, and  $E$  is a matrix containing random errors,  $Y$  is the input grain-size distribution dataset, which consists of  $n$  grain-size distributions written as vectors of volumetric percentages increasing to 100% (Weltje, 1997).



This research utilised AnalySize Version 1.1.0 (Paterson and Heslop, 2015). Since AnalySize provides the most precise analysis, it is used to extract sediment grain size data (van Hateren et al. 2018). Utilising a non-negative matrix factorisation (akin to principal component analysis), the EM distributions and their abundances are generated periodically. Individual GSD is used to estimate the number of EMs based on the results of EM modelling (van Hateren et al. 2018).

### **3. Results**

#### **Coastal Hydrodynamics**

For the five years in focus, the average significant wave height ( $H_s$ ), wave period ( $T_p$ ), and wind speed for the NG (SG) coastal region were predicted to be 1.49 m (1.42 m) and 7.87 s (7.94 s), respectively (Fig 2). PRM and NEM months have a calmer wave climate than SWM months. The coastal region had more significant  $H_s$  (2.2 - 3 m) during the SWM, while the NEM and PRM had lower  $H_s$  (0.7-0.9 m). The wave period ranged between 6.5 and 7.7 seconds in PRM, 8.9 and 9.3 seconds in SWM, and 6.8 and 8.6 seconds in NEM.

Winds in the region are predominantly southwesterly, northeasterly, and north-westerly in July, November, and April (Fig 2). NG and SG had stronger winds of 6–8 m/s and 5–7 m/s during the SW monsoon. NG experienced winds within the range of 3–5 m/s in PRM and NEM, while SG had 2–4 m/s during NEM (Fig 2).

Additionally, significant peaks in wind speed and  $H_s$  were observed in June 2019 (orange circle) and October 2019 (purple circle) (Fig 2), depicting tropical cyclones Vayu and Kyarr are a representation of episodic events typical of the west coast of India.

From 2016 to 2018, the MDV and ZR rivers discharged at high rates during the SW Monsoon (238.67 m<sup>3</sup>/s and 24.82 m<sup>3</sup>/s) and lower rates during the NE Monsoon (13.524 m<sup>3</sup>/s and 1.553 m<sup>3</sup>/s; data extracted from India Water Resources Information System database).

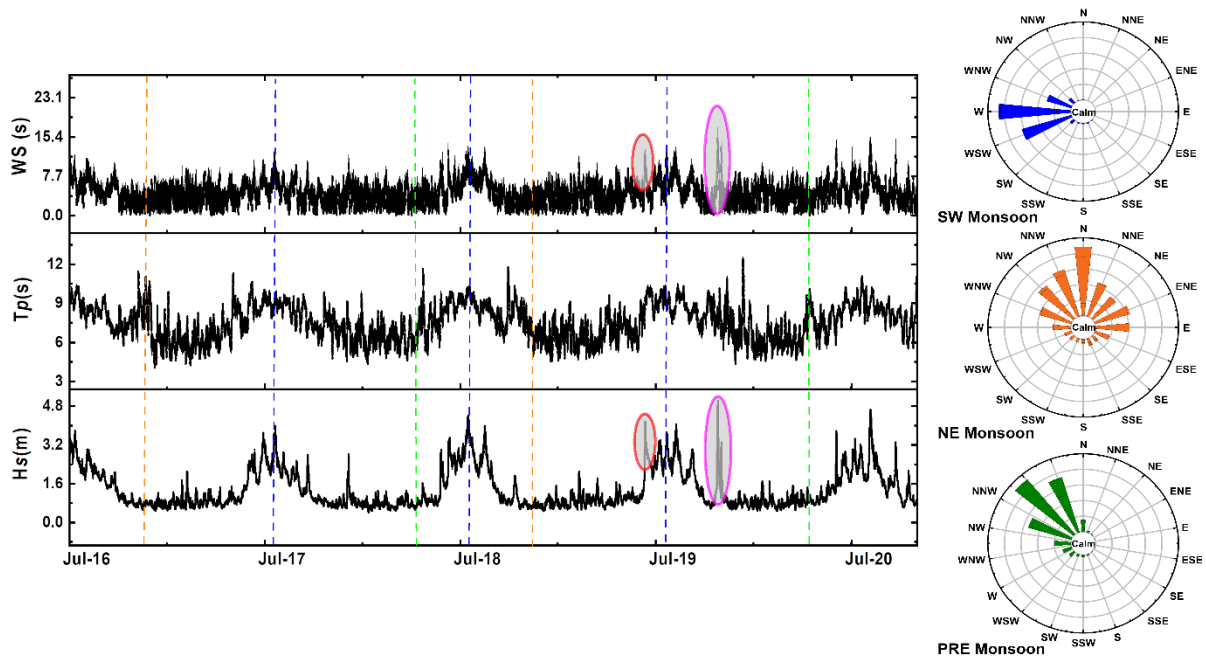


Fig 2 —2016 – 2020 hydrodynamic trend for the coastal region of Goa. Left: Significant wave height (Hs), Wave period (Tp), and Wind speed (m/s). Dashed lines: blue (SWM), green (PRM) and orange (NEM). Circles (orange: cyclone **Vayu**; purple: cyclone **Kyarr**). Right: Average wind direction ( $^{\circ}$ ) for the SWM, NEM and PRM

## End Member modelling of Grain Size Distributions

### Estimating End Members

Goa's coast sediments for all seasons are characterised by a wide range of particle sizes, between  $31.25 \mu\text{m}$  to  $2\text{mm}$ , indicating a medium-grained, sandy to silty texture (Fig. 3a, 4a, 5a). As a result of the variable size classes, the GSD datasets are processed using EMMA. We used the AnalySize Software following Paterson and Heslop's (2015) definition of a good fit to calculate the coefficient of determination ( $R^2$ ) and the angular distance in degrees (Theta) based on the grain size data (i.e., if the  $R^2$  value is high and theta is low, then the fit is good). The goodness-of-fit statistics show a better fit (increasing  $R^2$ ) between the raw GSD spectrum and the EMs as the number of EMs increases (Table 2). We utilised a model with four EMs, which together explained 100% of the observed GSDs, to represent the entire data set. Mean modal size classes for these EMs are  $32 - 63 \mu\text{m}$  (EM1),  $63 - 125 \mu\text{m}$  (EM2),  $125 - 250 \mu\text{m}$  (EM3),  $250 - 500 \mu\text{m}$  (EM4), (Fig. 3b, 4b, 5b). Seasonal and spatial fluctuations in decomposed EMs collected from sediment data sets are illustrated in Figures 3–6.

## Seasonal Distribution of End Members

### SW Monsoon

The EMMA of grain sizes of surface sediment samples ( $n = 95$ ) during the SWM depicted a polymodal distribution (Fig 3a). The goodness-of-fit statistics and linear correlation is utilised to optimise the one to six EM model (Fig. 3b). The mean coefficient of determination for the one to six models is 0.99 (explaining 100% of the variance in the sample population) with angular deviation  $> 0.8^\circ$  for one to six EMs (Table 2; Fig. 3c, 3d). Given the opposing demands of parsimony (few EMs) and repeatability, the goodness-of-fit statistics suggest a four-end-member model. The EM structure with four-end-member loadings - EM1, EM2, EM3 and EM4, with dominant modes of 62.07  $\mu\text{m}$ , 87.78  $\mu\text{m}$ , 190.34  $\mu\text{m}$  and 426.32  $\mu\text{m}$ , and D50 of 61.31  $\mu\text{m}$ , 93.42  $\mu\text{m}$ , 185.62  $\mu\text{m}$ , and 466.29  $\mu\text{m}$ , respectively, was retrieved after the analysis to comprehend the grain-size variations better. The corresponding size classes for the derive. EMs are represented by coarse silt, very fine sand, fine sand, and medium sand for EM1, EM2, EM3 and EM4.

Table 2 —End-member statistics for the Goa beach stations for SWM, NEM, and PRM

	Statistics for one to six EM loadings			Selected End Members			
	Coeff. of Determination (R <sup>2</sup> )	Angular Dev. (°)	Variance (%)	1	2	3	4
<b>SWM</b>	0.99	0.8	100	<b>1</b>	<b>2</b>	<b>3</b>	<b>4</b>
EM modes[ $\mu\text{m}$ ]				62.0	87.7	190.3	426.3
D50 [ $\mu\text{m}$ ]				7	8	4	2
				61.3	93.4	185.6	466.2
				1	2	2	9
<b>NEM</b>	0.99	1.1	99.99		<b>2</b>	<b>3</b>	<b>4</b>
EM modes[ $\mu\text{m}$ ]				-	80.2	190.3	482.9
D50 [ $\mu\text{m}$ ]					1	4	7
					84.3	167.5	495.9
					5	1	3
<b>PRM</b>	0.99	0.8	100		<b>2</b>	<b>3</b>	
EM modes[ $\mu\text{m}$ ]				-	86.7	165.3	-
D50 [ $\mu\text{m}$ ]					7	2	
					92.0	170.0	
					7	3	

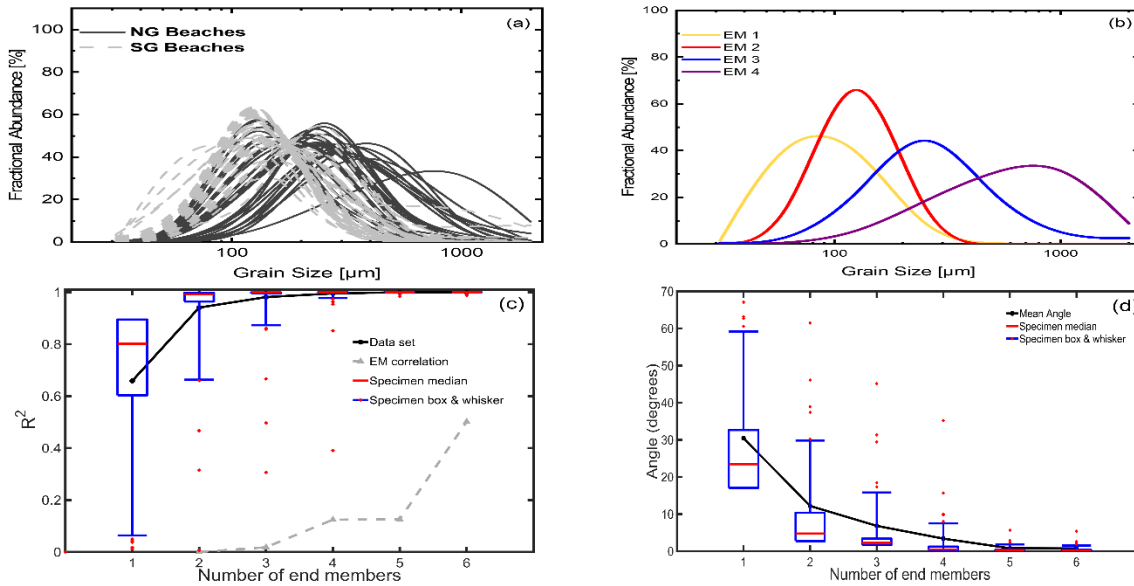


Fig 3 –EMMA results of grain-size data from the north and south Goa beaches during SWM (a) multiple grain size frequency distribution. (b) Densities of the modelled EMs (c) Coefficients of determination ( $R^2$ ) for each size class of models with 1 to 6 EMs. (d) Angular differences (in degrees) between the modelled and observed data for 1 to 6 EMs.

### NE Monsoon

Surface sediment samples during the NEM season ( $n=75$ ) revealed a polymodal distribution (Fig. 4a). The goodness-of-fit statistics for this season show an overlapping 3-EM model (Fig. 4b). The average coefficient of determination is 0.99 (i.e., 99.9 % accounting for total sediment population variance) with an angular deviation of  $1.1^\circ$  for a one to six EM model (Table 2; Fig. 4c, 4d). The retrieved EMs – EM2, EM3, and EM4, corresponding to very fine sand, fine sand and medium sand classes have dominant mean modes of  $80.21 \mu\text{m}$ ,  $190.34 \mu\text{m}$ ,  $482.97 \mu\text{m}$ , with the corresponding D50 of  $84.35 \mu\text{m}$ ,  $167.51 \mu\text{m}$  and  $495.93 \mu\text{m}$ .

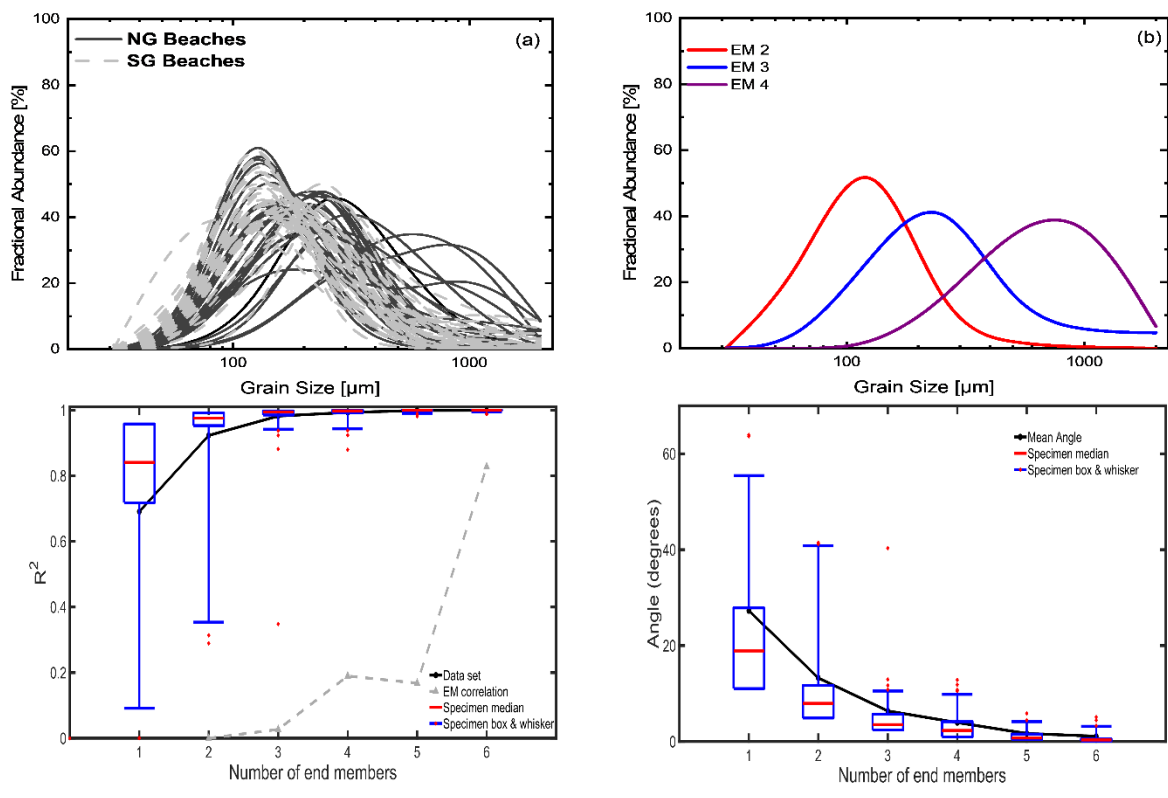


Fig 4 —EMMA results of grain-size data from the north and south Goa beaches during NEM (a) multiple grain size frequency distribution. (b) Densities of the modelled EMs (c) Coefficients of determination ( $R^2$ ) for each size class of models with 1 to 6 EMs. (d) Angular differences (in degrees) between the modelled and observed data for 1 to 6 EMs.

### Pre-Monsoon

In PRM, the surface sediments ( $n=57$ ) revealed a polymodal distribution (Fig. 5a). The discretised EMs for this season - EM2 (very fine sand) and EM3 (fine sand) (Fig. 5b) have dominant mean modes of  $86.77 \mu\text{m}$  and  $165.32 \mu\text{m}$  and corresponding median diameters ( $D_{50}$ ) of  $92.07 \mu\text{m}$  EMs  $170.03 \mu\text{m}$ . The goodness-of-fit statistics derived for the season from one to six end-member models ( $R^2 > 0.9$ , angular deviation  $> 0.2^\circ$ ; Table 2; Fig. 5c, 5d).

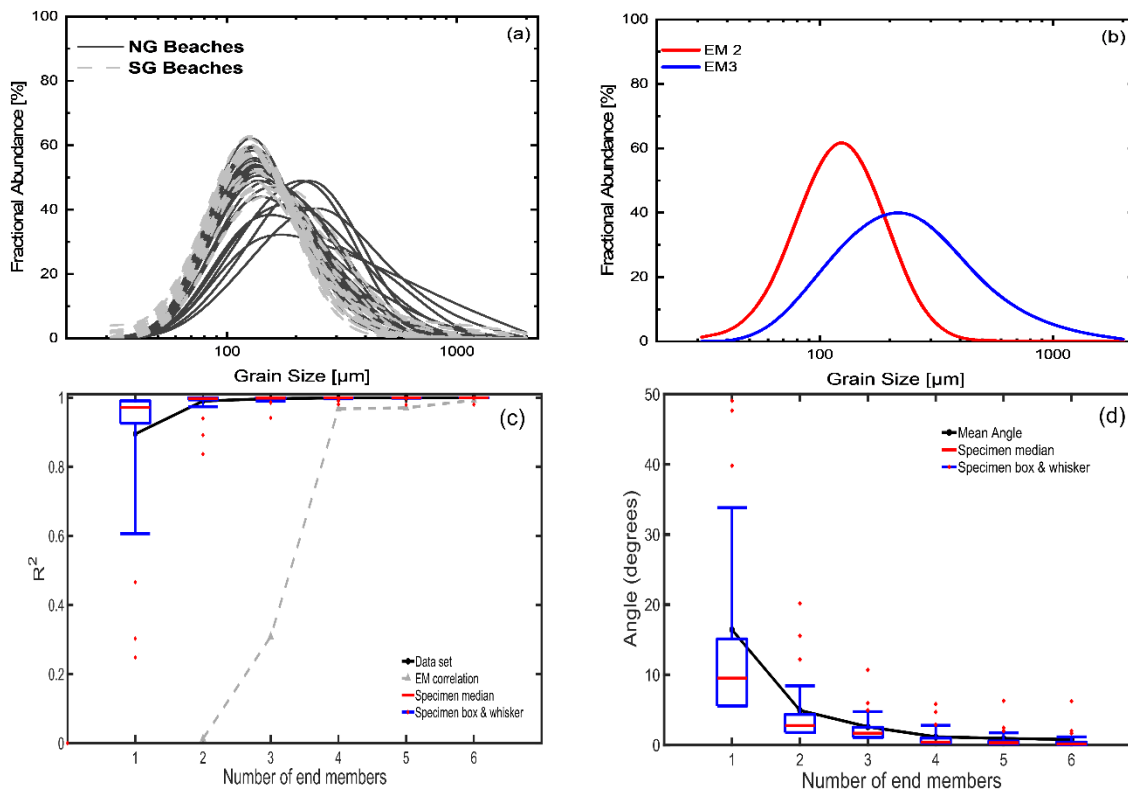


Fig 5 —EMMA results of grain-size data from the north and south Goa beaches during PRM (a) multiple grain size frequency distribution. (b) Densities of the modelled EMs (c) Coefficients of determination ( $R^2$ ) for each size class of models with 1 to 6 EMs. (d) Angular differences (in degrees) between the modelled and observed data for 1 to 6 EMs.

### Spatial Distribution of End Members along Goa Coast

The spatial distribution of sediment set EMs illustrated in Fig. 6 and Table 3 shows the spatial distributions of the relative abundance (%) of the four decomposed EMs. SG beach sediments (VEL-MOB) are finer than NG beach sediments (BAGA-SINQ). The relative concentrations of EM2 and EM3 are the most abundant on all the beaches.

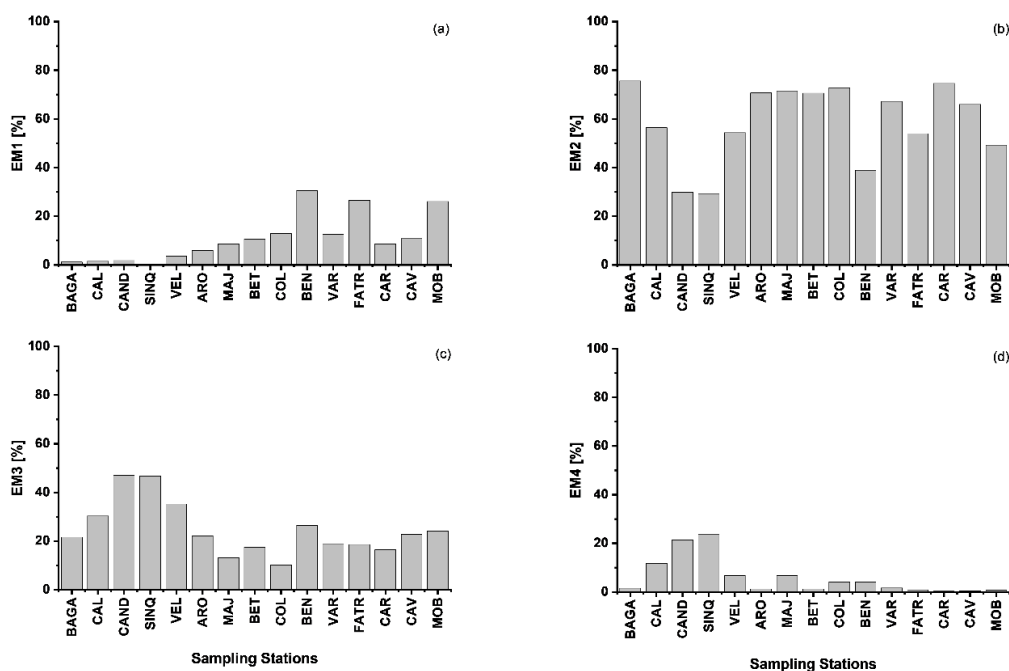
The largest concentrations of EM1 occur between SG 1 and SG 11, ranging from 3.6% to 30.56%, with notable peaks at SG 6, SG 8, and SG 11, ranging from 26.16 % to 30%. NG (1, 2) and NG (7, 8) exhibited the lowest relative EM1 concentration (<2%; range: 0.4-1.8 %). The most prevalent EM along the coast is EM2. Relative contents between NG (1, 2) and NG (7, 8) depict a decreasing southward trend, with NG (1, 2) having 75.6% and NG (7, 8) at 29.3%. Except for SG 6 and SG 11, which have lower relative contents of 38.9 and 49.2 %, the distribution of SG beaches is relatively uniform, ranging between 53.9% and 74.6%.

EM3 exhibits significant availability along the coast of Goa. The relative concentrations of NG (1, 2) and NG (7, 8) exhibit an increasing southward trend within the range of 21.6 and 47.1%, with NG (5, 6) and NG (7, 8) exhibiting high peaks. In contrast, the SG sector had relative contents ranging from 10.2 to 35.3%, with a peak distribution in SG 11 (35.3 %). EM4 is the rarest EM along the coast. The NG stretch of beaches depicts an increasing southward trend from 1.6% to 23.6%, with a maximum in NG (7, 8). In contrast, the SG beaches exhibit a negligible distribution of this EM, with peaks at SG 1 and SG 3 (0.3% -6.8%; average content: ~6.75 %).

Table 3 –Relative abundance (%) of the four EMs of the beach sediments along the Goa coast.

Beach Sample Stations		EM1 (Coarse Silt)	EM2 (Very Fine Sand)	EM3 (Fine Sand)	EM4 (Medium Sand)
BAGA	NG 1&2	1.2	75.6	21.6	1.6
CAL	NG 3&4	1.5	56.4	30.3	11.8
CAND	NG 5&6	1.8	29.8	47.1	21.4
SINQ	NG 7&8	0.4	29.3	46.7	23.6
VEL	SG 1	3.6	54.3	35.3	6.8
ARO	SG 2	6.0	70.6	22.2	1.2
MAJ	SG 3	8.6	71.5	13.1	6.7
BET	SG 4	10.6	70.6	17.5	1.2
COL	SG 5	12.9	72.8	10.2	4.1
BEN	SG 6	30.5	38.9	26.4	4.1
VAR	SG 7	12.5	67.2	18.7	1.6
FATR	SG 8	26.6	53.9	18.6	0.9
CAR	SG 9	8.7	74.6	16.4	0.3
CAV	SG 10	10.8	66.0	22.7	0.5
MOB	SG 11	26.1	49.2	24.0	0.7

Fig 6 —Spatial distributions of the relative abundance of (a) of the beach sediments along the north and south Goa coast.



#### 4. Discussion

##### Spatio-temporal trends in EM distribution

The AnalySize algorithm identifies the number of subpopulations that may contribute to sediment GSDs to derive unimodal EMs (subpopulations) employing genetic data from GSDs (Paterson and Heslop, 2015). The variations in EMs correlate to alternative mechanisms that systematically affect the grain-size distribution as sediment is transported and deposited from its source region (Boulay et al., 2007; Prins et al., 2002).

Along the coast of Goa, we examine the impact of EM spatiotemporal signatures and EM subpopulation distribution on NG and SG beaches. The divergent tendencies of the derived EMs on the beaches of the Goa coast indicate that distinct processes influence their movement. The nearshore wave environment on India's central west coast is seasonal, resulting in seasonal fluctuations in mean grain size during the SWM (Neetu et al. 2006; Shetty and Jayappa 2020; Vethamony et al. 2009). Significant wave height contributes to coastal erosion by accelerating the transport of coastal sediment (Kunte et al. 2014a; Kumar et al. 2003). As a result, the amount of beach material eroded varies with wave height (Doukakis 2005). Fig 2 shows consistent wave heights and periods, with peak values during the SWM. These findings support ERA5 wave height ( $H_s$ ) and period ( $T_p$ )



statistics showing that the NEM had lower values than the SWM. The Goa coastline is categorised as moderate risk (Kumar et al. 2006) since the tidal range is relatively stable throughout the year, except during the SWM, the primary and significant winds blow onshore, generating cyclonic disturbances, which in turn modifies the coastline (Veerayya, 1972; Shanas and Kumar, 2014). Van Rijn et al. (2001) assert that waves regulate sediment processes on sandy beaches.

In Figs. 3b, 4b, and 5b, the surface distributions of the four-grain size derived EMs resulting from clastic sediment populations are represented for the SWM, NEM and PRM. Similarly, Figs. 6a – d and Table 3 depict the spatial distribution on the beaches along the Goa coast. These plots demonstrate significant spatio-temporal trends that can be interpreted to reflect recent climatic changes along the central west coast of India, specifically in the Goa region.

Significantly, the observed temporal variation in SWM demonstrates an overall strong relationship with the reported history of morphodynamic and hydrodynamic interactions along the coast of Goa (Kunte et al., 2014a; Loveson et al., 2014; Shetty & Jayappa, 2020; Wilson et al., 2014). Due to the enhanced wind and wave regime of SWM (Kumar et al. 2017), the relative abundance of coarse silt (EM1) in the record along the coast, particularly in the SG region (Fig. 6a), generally follows the deposition via sediment turbulent flows characteristic of this season. The highest EM1 abundances are found at the SG beaches, with values up to ~26% following a gradual southward increasing trend (Fig. 6a). While this trend may not support the coastal transport pathway of the SWM season (Jayakumar et al. 2001), we infer that this EM proxy is likely from distal sources, most probably the southern Sal river which lies adjacent to the SG 11 beach (with EM1 abundance = ~26 %; Table 3). However, there is a rapid decrease in EM1, with negligible proportions between NG 1 and NG 8 (below 2%; Table 3). We interpret this variable trend as resulting from transport due to the interaction between tidal currents and other coastal processes that define selective sorting, winnowing, and conveying material along the Goa coast, indicating estuary-beach sediment exchange via overland runoff (Oyedotun, 2016) and other viable sources including eroded materials from the adjacent coastal area. This is synonymous with the hydrodynamic condition during SWM (Fig 2). Karlekar (2015) reports a narrow beach width in SWM, accompanied by variable sediment sizes owing to a complex hydrodynamic regime. According to Kumar et al. (2012), an increase in wave height, particularly in SWM, leads to increased wave energy, resulting in increased shoreline erosion. Kunte et al. (2014a) have described this coastline's erosional risk, highlighting the erosion-prone zones to support this view. Their study revealed that NG beaches have a gentle slope ( $0.1^\circ$  -  $0.3^\circ$ ) and have a medium erosional risk. Similarly, they reported southern part of SG beaches (SG 4

to SG 11), with a steeper slope ( $>0.3^\circ$ ), had a significant erosional risk, while the northern part of SG beaches is vulnerable to storm and sea level rise due to low coastal slopes ( $<0.1^\circ$ ).

Considering the distinct patterns of temporal variation found in the other elastic EMs (Figs. 4b and 5), the SWM mechanism appears to have solely influenced the silts of EM1. We hypothesise that the influence of SWM on the influx of these particle populations and their final delivery to the beaches was outweighed by the high energy controls characteristic of this season. The SWM impacts significantly in this environment are evident by high energy levels and increased river discharge compared with NEM and PRM. Studies by Sahu (1964) and other earlier studies have assumed a widely accepted analogy that fine sediments are winnowed during high-energy events leaving behind coarser materials. However, this view does not support the presence of EM 1 (coarse silt), the finest grain size class of the extracted EMs. Hence the actual source of this EM cannot be solely linked to river discharge, as we can also assume a contribution from headland weathering and erosion or deposition from distal sources. The latter may be likely considering the decreasing trend of the EM from NG (5, 6) to NG (1, 2). We can explain that with the Sinquerim Fort at NG 8, deposition of likely weathered EM1 is not favoured, and these materials are thereby deposited via currents northward to the adjacent NG beaches. The low occurrence of this EM suggests that the coastline is susceptible to erosion by climatic and coastal processes.

EM2 and EM3 are dominant EMs found in all seasons and reach their peak percent-abundance proportions during SWM (Fig. 3b, 4b, 5b) and across all the studied beaches (Fig. 6b, 6c). We interpret the abundance of EM2 and EM3 in the three seasons to indicate the contemporary nature of the sediments, probably the interaction of the paleo-shoreline (Sahu 1964) with modern sediments deposited from proximal sources (including river discharge) through the action of swash and backwash and associated currents along the beaches. This implies that these detrital sediments from variable sources likely represent changes in the prevalence of estuarine runoff transport (Ganesh et al., 2013; Hegde et al., 2004; Niraj et al., 2015; Shetye et al., 2007) or processes of post-depositional sediment redistribution within the coast and are however not subject to seasonal climatic influences. Mascarenhas (1998) states that most preserved sediments along the beaches result from collapsed dune materials following increased eco-tourism and human activities along the south Goa region. The SG stretch of beaches is semi-embayed between headlands. The beaches are primarily low-angled with a history of sand-dune morphology (Mascarenhas, 1998b, 1999). Hence, this semi-protected geomorphic structure also gives credence to preserving the fine sand EMs (EM1, EM2, and EM3) in the SG sector.

Different mechanisms might control changes in the (relative) quantity of EMs along the coast. First, SWM may accelerate the influx of fine sand sediment from estuarine runoff, followed by coastal erosion along the southern axis of the beach and deposition in the northern direction. (Jayakumar et al. 2001; Seelam et al. 2014). This is because strong winds can resuspend the bottom material, and the current speed is adequate to carry the sandy particles by saltation and suspension (Lamy et al., 2015; McCave and Andrews, 2019; McCave and Hall, 2006; Chen et al., 2013). Inversely, during NEM, eroded materials are transported and redeposited southwards (Jayakumar et al. 2002). The absence of the finer EM1 indicates winnowing and subsequent erosion at the onset of NEM, leaving EM2, EM3, and EM4 (Fig. 4b). The continuous erosion during NEM, as inferred from the rapid and prominent decline in EM4 abundance shortly after the start of the PRM (Fig. 5b). Hence, we can surmise that EM 2 and EM 3 which are prevalent during PRM represent the fractions that climatic drivers do not influence. This view is supported by the spatial prevalence on all the beaches (Fig 6b and 6c). These episodes of synchronous erosion, redistribution, and redeposition are evident in the preservation of the EM2 and EM3 in the coast's sediments in an entire climatic cycle. As Dietze & Dietze (2019) and Jovivek & Chandrasekar (2017) note, the insufficient separation of the two respective source populations of fine and very fine fractions by the EM modelling may also contribute to the similarity with trends in EM 2 and EM3 across the seasonal cycle.

The coarse-grained EM4 fraction is the least abundant of the four clastic EM fractions (Fig. 6d). To explain the occurrence of this EM, we examine two likely scenarios: (i) a reflection of erosional input from the headlands during SWM. (ii) a representation of the prevalence of coarser fractions as a response to an erosional setting that washes away the fine and very fine sands fractions due to an increase of energy in waves and wind regime of the SWM and redistribution during NEM. EM4 proxy distribution in the first scenario is consistent with Karlekar's (2015) views suggesting a possible contribution of weathered headland material to the coastal beaches of Goa during intense wave activities in SWM. As seen in Fig 6d, it is observed that though this EM proxy is found in low concentrations along the coast (table 3), it has significant peaks in NG (7, 8) and SG 1, which are close to the adjacent headlands. However, the highest proportions of EM4 occur during NEM, which can be attributed to when redistribution occurs after erosional activities characteristic of SWM (Fig 4b). These findings, however, contrast with past assumptions suggesting an extensive SWM erosion and NEM deposition. For example, a study by Rajasekaran et al. (2014) showed that beaches in Goa erode during the SWM and accrete during the non-monsoon (PRM and NEM). Their research also found that morphological changes in NG (3, 4) and SG 5 have an annual cycle with the most significant sediment deposit in PRM. The researchers suggest that low-energy wave regimes during

the NEM and PRM help slow down beach erosion induced by the SWM. In contradiction to their views, the spatio-temporal distribution of retrieved EMs in this study reveals the interchangeable erosion and deposition events in both SWM and NEM. Studies by Jayakumar et al. (2001, 2002), Seelam et al. (2014), and Kunte et al. (2014a) give credence to these views with insight into longshore transport pathways along this coast. It is, however, not conclusive, using only grain size to attribute primary sources without information on their mineral composition. Hence, this study is an index study to guide more extensive research and trace a proper sediment transport pathway for this region.

### **Source sediment contributions**

Modern sedimentary patterns, which Weltje & Prins (2007) termed dynamic populations, result from sedimentary sources and hydrodynamics; hence geologists compare the grain size of EMs to proximal sources (van Hateren et al. 2018). Although grain sizes vary between provenance regions, Due to dynamic environmental conditions, GSDs can be detected in numerous sedimentary sources with overlapping ranges, making it hard to identify origin based on grain size (Yu et al. 2016; van Hateren et al. 2018; Meyer et al. 2020; de Mahiques et al. 2021; Liu et al. 2021).

EMMA can reflect a variety of sedimentary and hydrodynamic sources and settings to recover grain size information for sediments produced and influenced by varied dynamic populations. In order to gain a better understanding of the physical significance of the dynamic populations of unique EMs, this data includes information about the local dynamic sedimentary environment rather than relying on the broad descriptive assessments typically used when investigating dynamic sedimentary environments. As an alternative to clay-silt-sand triangulation diagrams, EMs distributions can more accurately portray distinct sediment ranges within sedimentary regions. This technique works well for the Goa coast because decomposed EM proportions can accurately characterise MDV and ZR estuary ranges and variations; thus, this methodology is selected for analysing provenance and sedimentary processes.

The estuaries MDV and ZR, which are bounded at the mouth by prominent headlands, drain about 69% of Goa's geographic area and significantly influence the beach platform, sediment transport and morphodynamics (Karlekar 2015). Annually, the MDV and ZR estuaries discharge detritus transported along the coast by longshore currents (Shah et al. 2020). The MDV and ZR rivers have significant discharge rates of 238.67 m<sup>3</sup>/s and 13.524 m<sup>3</sup>/s during the SWM and NEM. The considerable rainfall and heavy discharge that facilitates quick transport of weathered materials from these estuaries and other rivers along the central west coast of India during SWM has constantly

supplied sediments to India's central west coast (Murty et al. 1982; Sundar and Shetye 2005; Shetye et al. 2007). Aeolian inputs are reported to have a negligible effect on the sediment of the Goa coast (Shah et al. 2020). Granulometric variations in the MDV and ZR estuaries indicate the presence of the estuary's diverse flow pattern (Yasin et al. 2016). The differential sorting process of sediment transit as a result of fluctuating mean discharge, flow velocity, and seasonal variation, which results in polymodal grain distributions, can be employed to explain the variation in mixed sediment particle size in the deposited along the coast (Yasin et al. 2016; Kumar et al. 2017; Pradhan et al. 2022). Shetye et al. (2007) reported strong winds (4-7 ms<sup>-1</sup>) and wave periods (8 secs – 10 secs) and tidal currents (~2.5 ms<sup>-1</sup>), and heavy swells during SWM as the significant flocculation drivers for resuspension of sediments in MDV and ZR, which are transported to the coast and nearshore areas due to high discharge rate (Kessarkar et al. 2010; Fernandes et al. 2018).

In this regard, recent sediment samples in this coastal area were taken from 10 m depth in the nearshore sections of NG and SG and the MDV and ZR river estuaries for source assessment with average EM abundances from the three seasons. Due to few samples, we opted not to perform a separate end-member investigation on them. Table 4 summarises particle size distributions from these sources.

According to Fig. 7a, a potential sediment exchange interaction exists between EM1 (~62µm) and MDV-L (~52 µm) estuary mouth sediments, both of which belong to the coarse silt grain size class. Similarly, the primary mode of the bimodal MDV-M (~125µm) is closely related to the modal class of EM3 within the fine sand range (190µm). While MDV-M may be located at a more active part of the estuary, favouring fine sand (125µm), the occurrence of this size class represented by EM3 cannot be conclusively said to be from this source. This is because the abundance of finer sediments at MDV-L may not allow for the outflow of this EM to the coast; hence the source of this EM can only be verified through geochemical analysis and provenance analysis.

Table 4 —Particle size distribution of nearshore and estuarine sediment sources to the Goa coast

	D50 (µm)	Mean (µm)	Sorting	Skewness	Kurtosis
MDV-U*	12.24	14.03	3.93	0.11	0.98
MDV-M	237.81	125.01	4.61	-0.64	1.99
MDV-L	59.95	51.79	3.95	-0.18	1.01
ZR-U	13.70	15.72	3.63	0.08	0.79
ZR-M	42.72	45.18	6.98	-0.02	0.65
ZR-L	76.26	65.27	4.24	-0.21	0.93
NS-NG	4.35	4.93	-	-	-
NS-SG	4.42	5.12	-	-	-

\* Mandovi upper -MDV-U; Mandovi middle - MDV-M; Mandovi lower - MDV-L; Zuari upper - ZR-U; Zuari middle ZR-M; Mandovi lower - ZR-L; Nearshore North Goa - NS-NG; Nearshore South Goa - NS-SG

The EM dispersion is unaffected by MDV-U sediments. There is a correlation between the average mean modes of the EM2 (85  $\mu\text{m}$ ) and ZR-L (65  $\mu\text{m}$ ) deposits, which are composed of very fine sand, as shown in Fig. 7b. The bimodal ZR-M coarse silt mode correlates similarly with the lower EM1 mode, as is the case with the nearshore sediments ( $\sim 5\mu\text{m}$ ) depicted in Figure 7c, which performed poorly compared to the prescribed EMs around the coast. EM3 adequately represents the fine-grained bimodal subpopulations of the ZR-U and ZR-M sediments.

As shown by the grain size frequency curves (Fig. 3a, 4a, 5a), sediments are distributed over a broad spectrum of medium sands to coarse silt, and the selected end members depict this with representative peaks within this spectrum. Similarly, the bimodal populations discovered in MDV and ZR samples replicate the complicated sediment exchange between marine and estuarine environments (Lee et al. 2011). Figures 7a, b, and c demonstrate that the varied sediment sources are linked to riverine/inland and offshore sources. The relationship between EM1, EM2, and EM3 to MDV and ZR lower estuary deposits can be attributed to the SWM's enhanced ebb-tidal discharge, which transports a vast proportion of sand-sized materials combined with weathered sediments from the river drainage basin to the coast as unconsolidated sediments (Shetye et al. 2007; Kessarkar et al. 2010; Fernandes et al. 2018).

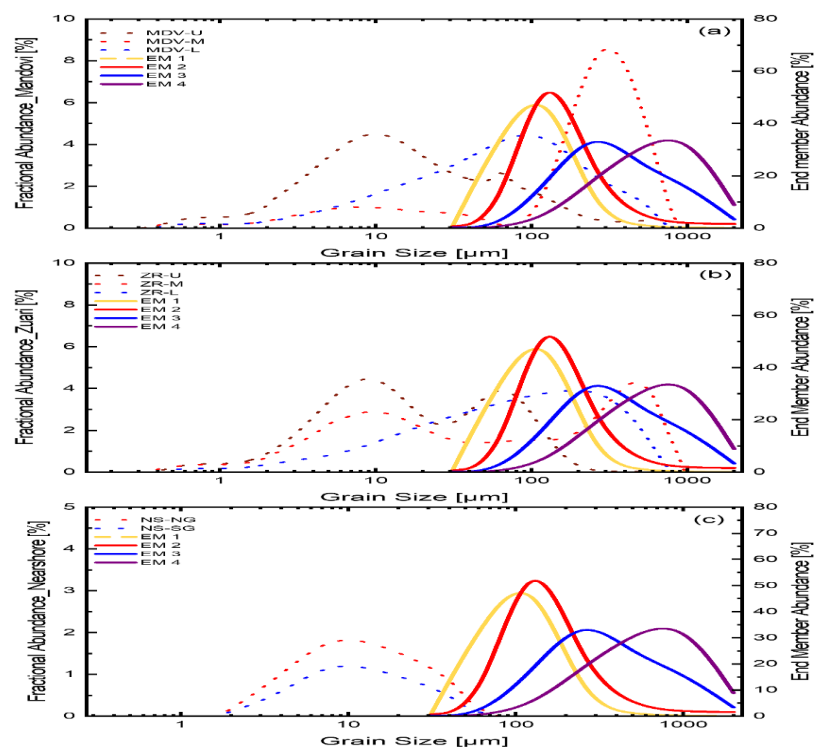


Fig. 7 —Overlay plot of the grain-size distributions (GSDs) of representative source sediments (a) MDV sediments (n =3) (b) ZR sediments (n =3) (c) Nearshore sediments (n =2). The plot of all observed GSDs (dotted lines) of the source sediments overlain with the three-season average of the four retained EMs (coloured straight lines), explaining 99.9% of the variance in the beach sediment datasets.

Deepti et al. (2007) reported considerable monsoonal deposition of fines (clay and silt) from the MDV and ZR rivers due to the prevailing ebb tidal asymmetry of the river. Previous research suggests that the net longshore drift, which is northerly during SWM, and southerly in NEM, is responsible for transporting these EMs along the coast (Neetu et al. 2006; Seelam et al., 2014; Shanas & Sanil Kumar, 2014b). However, there is a paucity of information regarding net longshore trends along this coast during PRM.

EM4, the coarser end of the represented size classes, can be linked to weathering of the headlands (Karlekar, 2015; Wilson et al., 2014) and short-distance travel from the source to the coastline through combined wave refraction and longshore current. Their prevalence along the beaches, particularly in NG (7, 8) and SG 1 attributed to their proximity to headlands (Fig. 6d). Consequently, it can be inferred that these EMs reflect changes in the transport capacity of inflowing rivers as well as hydrologic events related to wind/wave erosion or an increase in the vicinity of the sediment source. The EM distributions further corroborate the concept that the sedimentary regime along this coast is controlled by the sediment transport capacity of inflowing streams due to their increased velocity and discharge.

It is important to note that beach slope changes can transport sediment from nearshore bottom areas (where most discharged materials settle first) to the coast. The occurrence of such beach slope alterations has been recorded by Loveson et al. (2014), who also related the alteration of the beach slope to seasonal variations. This occurrence is not included in the present discussion because the clay-like sediments from the nearshore (NS-NG and NS-SG) did not correspond with the derived EMs (Fig 7c). However, if the nearshore area is considered a temporary source during SWM or at the peak of episodic events, such as cyclones, perhaps EM1 can be seen as a product of the mixing of nearshore mud with beach sands

Erosional and depositional evidence abounds for SWM and NEM in the distribution of EMs. The study suggests that the transportation and depositional processes of the surface sediments along the coast are controlled by the hydrodynamic process operating in these sub-environments. This investigation generated well-resolved EM seasonal and spatial limits, and the results are more

reasonable and reliable than classifications based on sediment type or sediment content from previous research.

Since the bulk of sediments deposited on these beaches cannot be conclusively attributed to discharged materials from the rivers, considering that most of the transported material may be deposited in pocket beaches surrounding the headlands. Hence we suggest a contribution of deposited material from distal sources via longshore transport, with more evidence from geochemical studies, which can be applied to different coastal settings over varied regional scales.

## **5. Conclusion**

The surface sediment component of a five-year record of Goa's coast gives valuable information on process-driven environmental changes. This study aims to understand better ocean–coastal–fluvial/hinterland interactions in India's Central West coast. The southwest monsoon controls rainfall in the sediment source region, driven by climate variability.

We provide a non-parametric end-member algorithm. By merging several EMMA iterations with similar probabilities, we identified resilient sediment components from an existing detrital system on the Goa coast. In each statistically robust EM, a discrete particle population linked with a particular sort of contemporary source material is shown. EMMA detected four substantial grain-size EMs indicating the coarse silt (EM1), very fine sand (EM2), fine sand (EM3), and medium sand (EM4) classes.

The highest variability of the beach sediments is evident during stormy coastal conditions in SWM when beaches receive sediment from waves of high steepness and significant river drainage from MDV and ZR. The occurrence of EM4 in NEM suggests that this season's calm coastal conditions do not support the resuspension of fines or winnowing activities but are likely indicative of erosion of fine and very fine sand at the NG beach arch during SWM, with no recovery of fine sediment materials during NEM. Similarly, the absence of EM1 and EM4 during PRM suggests a period of no deposition and erosion. The prevalence of sediment variability within the decomposed EMs suggests continuous reworking, depicting the flow characteristics and high-energy environment. Only two components of our beach system remain constant, namely the very fine sand and fine sand EMs, inferred to be contemporary beach sediments.

This study shows that EMMA can identify diverse EMs that directly represent sedimentary sources and infer spatiotemporal patterns compared to standard approaches to investigating dynamic environments that rely on sediment grain size-types or contents. EMs with stronger connections to sedimentary sources can more precisely depict local and regional sedimentary settings and have



significant theoretical and practical implications. These results give a quantitative measure for evaluating the response of sediment particle size to sediment provenance and sedimentary environment dynamics. It also lays a foundation for more detailed long-term data collection with a deeper look into the geochemical constituents in the source samples and EMs. Hence, to further improve EM modelling, adding grain-size components and geochemical data for specific grain-size fractions will aid in understanding sediment dynamics and defining sediment proxies for tracing a proper interseasonal sediment transport pathway. Understanding sediment along Goa's coast will help develop coastal management strategies.

### **Conflict Of Interest**

The authors declare that they have no conflict of interest.

### **References**

- Ahmed E (1972) Coastal Geomorphology of India. Orient Longman, New Delhi
- Alharbi O, Williams A, Philips M, Thomas T (2016) Textural Characteristics of Sediments along the Southern Red Sea Coastal Areas, Saudi Arabia. Arab J Geosci 9:. <https://doi.org/https://doi.org/10.1007/S12517-016-2741-y>
- Amrutha MM, Sanil Kumar V, Sharma S, et al (2015) Characteristics of shallow water waves off the central west coast of India before, during and after the onset of the Indian summer monsoon. Ocean Eng 107:259–270. <https://doi.org/10.1016/J.OCEANENG.2015.07.061>
- Angusamy N, Rajamanickam G (2006) Depositional Environment of Sediments along the Southern Coast of Tamil Nadu, India. Oceanologia 48:87–102
- Anithamary I, Ramkumar T, Venkataraman S (2011) Grain Size Characteristics of the Coleroon Estuary Sediments, Tamilnadu, East Coast Of India. Carpathian Jour Earth Envi Sci 6:151–157
- Anoop T, V SK, Shanas P, Johnson G (2015) Surface wave climatology and its variability in the North Indian Ocean based on ERA-interim reanalysis. J Atmos Ocean Technol 32:1372–1385. <https://doi.org/10.1175/JTECH-D-14-00212.1>
- Aparna M, Shetye S, Shankar D, et al (2005) Estimating The Seaward Extent Of Sea Breeze From Quikscat Scatterometry. Geophys Res Lett 32:L13601. <https://doi.org/10.1029/2005gl023107>
- Bagnold R (1954) The Physics of Blown Sand and Desert Dunes. Methuen, London
- Bascom W (1951) The relation between sand size and beach face slope. Trans Am Geophys Union 32:866–874
- Bhat M, Chavadi V, Hegde V (2002) Morphological And Textural Characteristics of Kudle Beach, Karnataka, central West coast of India. J GeolSoc India 59:125–131
- Blott S, Pye K (2001) Gradistat: A Grain Size Distribution And Statistics Package For The Analysis Of Unconsolidated Sediments. Earth Surf Process Landf 26:1237–12:26:1237–1248

- Boulay S, Colin C, Trentesaux A, et al (2007) Sedimentary Responses To The Pleistocene Climatic Variations Recorded In The South China Sea. *Quat Res* 68:162–172
- Central Ground Water Board (CGWB) (2013) Ministry of Jal Shakti, Department of Water Resources, River Development and Ganga Rejuvenation, Government of India.
- Chandramohan P, Anand NM, Nayak BU (1992) Surfzone dynamics of the Konkan coast, India. *Oceanogr Indian Ocean*
- Chandramohan P, Kumar SJ, Kumar VS, Ilangoan D (1998) Fine particle deposition at Vainguinim tourist beach, Goa, India. *J Coast Res* 14:1074–1081
- Chempalayil SP, Kumar VS, Dora GU, Johnson G (2014) Near shore waves, longshore currents and sediment transport along micro-tidal beaches, central west coast of India. *Int J Sediment Res* 29:402–413. [https://doi.org/10.1016/S1001-6279\(14\)60054-8](https://doi.org/10.1016/S1001-6279(14)60054-8)
- de Mahiques MM, y Goya SC, Matos MC da SN de, et al (2021) Grain-size end-members and environmentally sensitive grain-size components: A comparative study in the mud shelf depocenters off southern Brazil. *Int J Sediment Res* 36:317–327. <https://doi.org/10.1016/j.ijsrc.2020.07.004>
- Deepti VG, Dessai, AG, Nayak GN (2007) Seasonal Distribution of Surface Sediments and Hydrodynamic Conditions in Zuari Estuary, Goa, Central West Coast of India. 26:25–32
- Dholakia A, Desai N, Deota B (1995) National Seminar On Recent Researches In: Geology Of Western India. In: Desai N, Ganapathi S (eds). pp 219–224
- Diekmann B, Kuhn G (1999) Provenance and dispersal of glacial-marine surface sediments in the Weddell Sea and adjoining areas, Antarctica: Ice-rafting versus current transport. *Mar Geol* 158:209–231. [https://doi.org/10.1016/S0025-3227\(98\)00165-0](https://doi.org/10.1016/S0025-3227(98)00165-0)
- Dietze E, Dietze M (2019) Grain-size distribution unmixing using the R package EMMAgeo. *E&G Quat Sci J* 68:29–46. <https://doi.org/10.5194/egqsj-68-29-2019>
- Dietze E, Hartmann K, Diekmann B, et al (2012) An end-member algorithm for deciphering modern detrital processes from lake sediments of Lake Donggi Cona, NE Tibetan Plateau, China. *Sediment Geol* 243–244:169–180. <https://doi.org/10.1016/j.sedgeo.2011.09.014>
- Dietze E, Maussion F, Ahlborn M, et al (2014) Sediment transport processes across the Tibetan Plateau inferred from robust grain-size end members in lake sediments. *Clim Past* 10:91–106. <https://doi.org/10.5194/cp-10-91-2014>
- Dietze E, Wünnemann B, Hartmann K, et al (2013) Early to mid-Holocene lake high-stand sediments at Lake Donggi Cona, northeastern Tibetan Plateau, China. *Quat Res (United States)* 79:325–336. <https://doi.org/10.1016/j.yqres.2012.12.008>
- Doukakis E (2005) Coastal Vulnerability and Risk Parameters. *Eur Water* 11:3–7
- Dwarakish GS, Vinay SA, Natesan U, et al (2009) Coastal vulnerability assessment of the future sea level rise in Udipi coastal zone of Karnataka state, west coast of India. *Ocean Coast Manag* 52:467–478. <https://doi.org/10.1016/j.ocecoaman.2009.07.007>

- Fernandes LL, Rao VP, Kessarkar PM, Suresh S (2018) Estuarine turbidity maximum in six tropical minor rivers, central west coast of India. *Hydrol Res* 49:1234–1254. <https://doi.org/10.2166/nh.2017.031>
- Fitch PJR, Lovell MA, Davies SJ, et al (2015) An integrated and quantitative approach to petrophysical heterogeneity. *Mar Pet Geol* 63:82–96. <https://doi.org/10.1016/j.marpetgeo.2015.02.014>
- Folk R (1971) LONGITUDINAL DUNES OF THE NORTHWESTERN EDGE OF THE SIMPSON DESERT, NORTHERN TERRITORY, AUSTRALIA, 1. GEOMORPHOLOGY AND GRAIN SIZE RELATIONSHIPS. *Sedimentology* 16:5–54. <https://doi.org/http://dx.doi.org/10.1111/j.1365-3091.1971.tb00217.x>
- Folk R, Ward W (1957) Brazos River Bar : A Study in the Significance of Grain-Size Parameters. *J Sediment Petrol* 27:3–26
- Ganesh B, Naidu AGSS, Rao JM, et al (2013) Studies on textural characteristics of sediments from Gosthani River Estuary-Bheemunipatnam, A.P., East Coast of India. *J Indian Geophys Union* 17:139–151
- Gerald M. Friedman (1967) Dynamic Processes and Statistical Parameters Compared for Size Frequency Distribution of Beach and River Sands. *SEPM J Sediment Res Vol.* 37: <https://doi.org/10.1306/74d716cc-2b21-11d7-8648000102c1865d>
- Glejin J, Sanil Kumar V, Balakrishnan Nair TM, Singh J (2013) Influence of winds on temporally varying short and long period gravity waves in the near shore regions of the eastern Arabian Sea. *Ocean Sci* 9:343–353. <https://doi.org/10.5194/os-9-343-2013>
- Goudie A (Ed. ). (1991) *Geomorphological Techniques*, 2nd Ed. Routledge
- Hamann Y, Ehrmann W, Schmiedl G, et al (2008) Sedimentation processes in the Eastern Mediterranean Sea during the Late Glacial and Holocene revealed by end-member modelling of the terrigenous fraction in marine sediments. *Mar Geol* 248:97–114. <https://doi.org/10.1016/j.margeo.2007.10.009>
- Hameed TSS, Kurian NP, Thomas K V., et al (2007) Wave And Current Regime Off The Southwest Coast Of India. *J Coast Res* 23:1167–1174
- Hartmann D (2007) From reality to model: Operationalism and the value chain of particle-size analysis of natural sediments. *Sediment Geol* 202:383–401. <https://doi.org/10.1016/J.SEDGEO.2007.03.013>
- Hegde, V. S. Kanchanagouri, D. Gosavi, P. T. Hanamgond, G. K. Huchchannavar G, Shalini, Bhat MS (2004) Depositional environment and silting in the Sharavati estuary, central west coast of India. *Indian. Jour Mar Sci* 33:296–302
- Heslop D, von Dobeneck T, Höcker M (2007) Using non-negative matrix factorisation in the "unmixing" of diffuse reflectance spectra. *Mar Geol* 241:63–78. <https://doi.org/10.1016/j.margeo.2007.03.004>

- Jayakumar S, Raju N, Gowthaman R, et al (2001) Daily beach profiles and littoral environmental observations off Baga, Calangute and Miramar beaches during February–March 1999. Dona Paula, Goa (India)
- Jayakumar S, Raju N, Gowthaman R, et al (2002) Daily beach profiles and littoral environmental observations off Baga, Calangute and Miramar beaches during November– December 1999. Dona Paula, Goa (India)
- Joevivek V, Chandrasekar N (2017) Data on nearshore wave process and surficial beach deposits, central Tamil Nadu coast, India. *Data Br* 13:306–311. <https://doi.org/10.1016/j.dib.2017.05.052>
- Karlekar S (2015) Beach response to natural headlands on South Konkan and Goa coast. *Transactions* 37:201–211
- Kessarkar PM, Rao VP, Shynu R, et al (2010) The nature and distribution of particulate matter in the Mandovi estuary, central west coast of India. *Estuaries and Coasts* 33:30–44. <https://doi.org/10.1007/s12237-009-9226-0>
- Konert M, Vandenberghe J (1997) Comparison of laser grain size analysis with pipette and sieve analysis: a solution for the underestimation of the clay fraction. *Sedimentology* 44:523–535
- Kumar VS, Shanass PR, Dora GU, et al (2017) Longshore sediment transport in the surf zone based on different formulae: a case study along the central west coast of India. *J Coast Conserv* 21:1–13. <https://doi.org/10.1007/s11852-016-0462-8>
- Kunte PD (1994) Sediment transport along the Goa-north Karnataka coast, western India. *Mar Geol* 118:207–216. [https://doi.org/10.1016/0025-3227\(94\)90084-1](https://doi.org/10.1016/0025-3227(94)90084-1)
- Kunte PD, Jauhari N, Mehrotra U, et al (2014a) Multi-hazards coastal vulnerability assessment of Goa, India, using geospatial techniques. *Ocean Coast Manag* 95:264–281. <https://doi.org/10.1016/J.OCECOAMAN.2014.04.024>
- Kunte PD, Jauhari N, Mehrotra U, et al (2014b) Multi-hazards coastal vulnerability assessment of Goa, India, using geospatial techniques. *Ocean Coast Manag* 95:264–281. <https://doi.org/10.1016/j.ocecoaman.2014.04.024>
- Kunte PD, Wagle BG, Sugimori Y (2001) Littoral transport studies along west coast of India - A review. *Indian J Mar Sci* 30:57–64
- Le Roux JP, Rojas EM (2007) Sediment transport patterns determined from grain size parameters: Overview and state of the art. *Sediment Geol* 202:473–488. <https://doi.org/10.1016/j.sedgeo.2007.03.014>
- Lee BJ, Toorman E, Molz FJ, Wang J (2011) A two-class population balance equation yielding bimodal flocculation of marine or estuarine sediments. *Water Res* 45:2131–2145. <https://doi.org/10.1016/j.watres.2010.12.028>
- Liu Y, Liu X, Sun Y (2021) QGrain: An open-source and easy-to-use software for the comprehensive analysis of grain size distributions. *Sediment Geol* 423:105980. <https://doi.org/10.1016/j.sedgeo.2021.105980>

- Loveson VJ, Gujar AR, Iyer SD, et al (2014) Beach dynamics and oscillations of shoreline position in recent years at Miramar Beach, Goa, India: A study from a GPR survey. *Nat Hazards* 73:2089–2106. <https://doi.org/10.1007/s11069-014-1175-7>
- Manoj NT, Unnikrishnan AS, Sundar D (2009) Tidal asymmetry in the mandovi and zuari estuaries, the west coast of India. *J Coast Res* 25:1187–1197. <https://doi.org/10.2112/08-1056.1>
- Mascarenhas A (1998a) Study of Goa and its environment from space: A report on coastal sand dune ecosystems of Goa: Significance, uses and anthropogenic impacts. National Institute of Oceanography, Goa. Retrievable from researchgate. net on, 21(06), p.2017.
- Mascarenhas A (1998b) Coastal sand dune ecosystems of Goa: significance, uses and anthropogenic impacts. Report, Environment of Goa from Space.
- Mascarenhas A (1999) The Coastal Regulation Zone of Goa: Oceanographic, environmental and societal perspectives. *Curr Sci* 77:1598–1605
- MASCARENHAS A (1998) Study of Goa and its Environment from Space. *Natl Inst Oceanogr*
- McLaren P, Hill SH, Bowles D (2007) Deriving transport pathways in a sediment trend analysis (STA). *Sediment Geol* 202:489–498. <https://doi.org/10.1016/J.SEDGEO.2007.03.011>
- Merkus H (2009) *Particle Size Measurements: Fundamentals, Practice, Quality*. Springer, Dordrecht
- Meyer I, Van Daele M, Tanghe N, et al (2020) Reconstructing East African monsoon variability from grain-size distributions: End-member modeling and source attribution of diatom-rich sediments from Lake Chala. *Quat Sci Rev* 247:106574. <https://doi.org/10.1016/j.quascirev.2020.106574>
- Murty CS, Veerayya M, Varadachari V (1982) Morphological Changes of the Beaches of Goa. II:35–42
- Nadaf FM (2019) Geographical Analysis of the Coastal Landforms of Canacona, Goa. *Int J Multidiscip* 4:655–661
- Neetu, S, Shetye, SR, Chandramohan P (2006) Impact of sea breeze on wind-seas off Goa, west coast of India. *J Earth Syst Sci* 115:229–234
- Niraj PS, Balaji R, Vethamony P (2015) Pre-monsoon hydrodynamic modeling of Goa coast, West coast of India. *ISH J Hydraul Eng* 21:276–286. <https://doi.org/10.1080/09715010.2015.1017747>
- Orpin AR, Woolfe KJ (1999) Unmixing relationships as a method of deriving a semi-quantitative terrigenous sediment budget, central Great Barrier Reef lagoon, Australia. *Sediment Geol* 129:25–35. [https://doi.org/10.1016/S0037-0738\(99\)00084-6](https://doi.org/10.1016/S0037-0738(99)00084-6)
- Orzech K (1997) Net shore drift of Goa coast, India. Western Washington University, Washington, U.S.A.
- Oyedotun TD. (2016) Sediment Characterisation in an Estuary-Beach System. *J Coast Zo Manag* 09:1–7. <https://doi.org/10.4172/2473-3350.1000433>

- Parthasarathy P, Ramesh G, Ramasamy, S., Arumugam, T., Govindaraj, P., Narayanan S, Jeyabal G (2016) Sediment Dynamics And Depositional Environment Of Coleroon River Sediments, Tamil Nadu, Southeast Coast Of India. *J Coast Sci* 3:1–7
- Passega R (1964) Grain size representation by CM patterns as a geologic tool. *J Sediment Res* 34:830–847. <https://doi.org/10.1306/74d711a4-2b21-11d7-8648000102c1865d>
- Paterson GA, Heslop D (2015) New methods for unmixing sediment grain size data. *Geochemistry, Geophys Geosystems* 16:4494–4506. <https://doi.org/10.1002/2015GC006070>
- Poizot E, Méar Y, Biscara L (2008) Sediment Trend Analysis through the variation of granulometric parameters: A review of theories and applications. *Earth-Science Rev* 86:15–41. <https://doi.org/10.1016/J.EARSCIREV.2007.07.004>
- Pradhan U, Mishra P, Mohanty PK (2022) Beach and nearshore sediment textural characteristics of a monsoonal wave–dominated micro-tidal, human perturbed environment, Central East Coast of India. *Arab J Geosci* 15:1–15. <https://doi.org/10.1007/s12517-022-09850-5>
- Prakash N, Ashly KU, Seelam JK, et al (2021) Investigation of nearshore processes along North Goa beaches: A study based on field observations and numerical modelling. *J Earth Syst Sci* 130:. <https://doi.org/10.1007/s12040-021-01755-3>
- Prins MA, Bouwer LM, Beets CJ, et al (2002) Ocean circulation and iceberg discharge in the glacial North Atlantic: Inferences from unmixing of sediment size distributions. *Geology* 30:555–558. [https://doi.org/10.1130/0091-7613\(2002\)030<0555:OCAIDI>2.0.CO;2](https://doi.org/10.1130/0091-7613(2002)030<0555:OCAIDI>2.0.CO;2)
- Prins MA, Postma G, Cleveringa J, et al (2000) Controls on terrigenous sediment supply to the Arabian Sea during the late quaternary: The Indus fan. *Mar Geol* 169:327–349. [https://doi.org/10.1016/S0025-3227\(00\)00086-4](https://doi.org/10.1016/S0025-3227(00)00086-4)
- Prins MA, Vriend M, Nugteren G, et al (2007) Late Quaternary aeolian dust input variability on the Chinese Loess Plateau: inferences from unmixing of loess grain-size records. *Quat Sci Rev* 26:230–242. <https://doi.org/10.1016/j.quascirev.2006.07.002>
- Prins MA, Weltje GJ (1999) End-Member Modeling of Siliciclastic Grain-Size Distributions: The Late Quaternary Record of Eolian and Fluvial Sediment Supply to the Arabian Sea and its Paleoclimatic Significance. *Numer. Exp. Stratigr. Recent Adv. Stratigr. Sedimentol. Comput. Simulations* 62:0
- Qasim SZ, Sen Gupta R (1981) Environmental characteristics of the Mandovi-Zuari estuarine system in Goa. *Estuar Coast Shelf Sci* 13:557–578. [https://doi.org/10.1016/S0302-3524\(81\)80058-8](https://doi.org/10.1016/S0302-3524(81)80058-8)
- Rajasekaran C, Kumar SJ, Gowthaman R, et al (2014) Sand spit and shoreline dynamics near Terekhol River mouth, Goa, India. *Indian J Geo-Marine Sci* 43:1311–1315
- Ramsey KW (1999) Beach Sand Textures From the Atlantic Coast of Delaware. Delaware Geol Surv Open File Rep No 41
- Sahu BK (1964) Depositional mechanisms from the size analysis of clastic sediments. *J Sediment Res* 34:73–83. <https://doi.org/10.1306/74D70FCE-2B21-11D7-8648000102C1865D>

- Sanil Kumar V, Anand NM, Chandramohan P, Naik GN (2003) Longshore sediment transport rate - Measurement and estimation, central west coast of India. *Coast Eng* 48:95–109. [https://doi.org/10.1016/S0378-3839\(02\)00172-2](https://doi.org/10.1016/S0378-3839(02)00172-2)
- Sanil Kumar V, Johnson G, Udhaba Dora G, et al (2012) Variations in nearshore waves along Karnataka, west coast of India. *J Earth Syst Sci* 121:393–403. <https://doi.org/10.1007/s12040-012-0160-3>
- Sanil Kumar V, Pathak KC, Pednekar P, et al (2006) Coastal processes along the Indian coastline. *Curr Sci* 91:530–536
- Seelam JK, Yadhunath EM, Jishad M, et al (2014) Post-monsoon equilibrium beach profiles and longshore sediment transport rates at Candolim, Miramar and Keri beaches of Goa, India. *Curr Sci* 106:408–416. <https://doi.org/10.18520/cs/v106/i3/408-416>
- Shah C, Banerji US, Chandana KR, Bhushan R (2020) <sup>210</sup>Pb dating of recent sediments from the continental shelf of western India: factors influencing sedimentation rates. *Environ Monit Assess* 192:. <https://doi.org/10.1007/s10661-020-08415-x>
- Shanas PR, Sanil Kumar V (2014a) Temporal variations in the wind and wave climate at a location in the eastern Arabian Sea based on ERA-Interim reanalysis data. *Nat Hazards Earth Syst Sci* 14:1371–1381. <https://doi.org/10.5194/nhess-14-1371-2014>
- Shanas PR, Sanil Kumar V (2014b) Coastal processes and longshore sediment transport along Kundapura coast, central west coast of India. *Geomorphology* 214:436–451. <https://doi.org/10.1016/J.GEOMORPH.2014.02.027>
- Shang Y, Beets CJ, Tang H, et al (2016) Variations in the provenance of the late Neogene Red Clay deposits in northern China. *Earth Planet Sci Lett* 439:88–100. <https://doi.org/10.1016/J.EPSL.2016.01.031>
- Shetty A, Jayappa KS (2020) Seasonal variation in longshore sediment transport rate and its impact on sediment budget along the wave-dominated Karnataka coast, India. *J Earth Syst Sci* 129:. <https://doi.org/10.1007/s12040-020-01504-y>
- Shetye SR, Dileep Kumar M, Shankar D, National Institute of Oceanography (India) (2007) The Mandovi and Zuari estuaries. 145
- Sundar D, Shetye SR (2005) Tides in the Mandovi and Zuari estuaries, Goa, west coast of India
- Suprit K, Shankar D (2008) Resolving orographic rainfall on the Indian west coast. *Int J Climatol Int J Clim* 28:643–657. <https://doi.org/10.1002/joc.1566>
- Titocan M, Ibitola M, Faleye B, Akinade-Solomon O (2018) Spatial Assessment of the Textural Characteristics and Sorting of Beach Deposits on the Barrier Lagoon Coastal Complex, Lagos Nigeria. *J Geol Geophys* 07: <https://doi.org/10.4172/2381-8719.1000334>
- Trivedi D, Raicy MC, Devi K, et al (2012) Sediment Characteristics of Tidal Deposits at Mandvi, Gulf of Kutch, Gujarat, India: Geophysical, Textural and Mineralogical Attributes. *Int J Geosci* 03:515–524. <https://doi.org/10.4236/ijg.2012.33054>

- Van Der Lubbe HJL, Frank M, Tjallingii R, Schneider RR (2015) Neodymium isotope constraints on provenance, dispersal, and climate-driven supply of Zambezi sediments along the Mozambique Margin during the past ~45,000 years. *Geochemistry, Geophys Geosystems* 181–198. <https://doi.org/10.1002/2015GC006080>
- van Hateren JA, Prins MA, van Balen RT (2018) On the genetically meaningful decomposition of grain-size distributions: A comparison of different end-member modelling algorithms. *Sediment Geol* 375:49–71. <https://doi.org/10.1016/j.sedgeo.2017.12.003>
- Veerayya M (1972) Textural characteristics of Calangute Beach sediments, Goa Coast (India). NISCAIR-CSIR, India
- Veerayya M, Murthy CS, Varadachari V. V. R (1981a) Wave refraction and littoral currents off Colva beach, Goa. *Indian J Mar Sci* 10:1–9
- Veerayya M, Murthy CS, Varadachari VVR (1981b) Sediment distribution in the offshore regions of Goa. *Indian J Mar Sci* 10:332–336.
- Veerayya M, Varadachari V (1975) Depositional Environments of Coastal Sediments of. *Sediment Geol* 14:63–74
- Vethamony P, Aboobacker AVM, Sudheesh AK, et al (2009) Demarcation of inland vessels' limit off Mormugao port region, India: a pilot study for the safety of inland vessels using wave modelling. 49:411–420. <https://doi.org/10.1007/s11069-008-9295-6>
- Wagle B (1993) Geomorphology of Goa and Goa Coast: A Review. *Mus Geol Di Bol*
- Weltje G, Prins M (2007) Genetically Meaningful Decomposition of Grain-Size Distributions. *Sediment Geol* 202:409–424.
- Weltje GJ (1997) End-Member Modeling of Compositional Data: Numerical-Statistical Algorithms for Solving the Explicit Mixing Problem 1
- Wilson JSJ, Sujitha SB, Shruti VC, et al (2014a) Seasonal variability of beach characteristics between Candoliam and Colva coast, Goa, India. *J Coast Sci* 1:33–40
- Wilson JSJ, Sujitha SB, Shruti VC, et al (2014b) Seasonal variability of beach characteristics between Candoliam and Colva coast, Goa, India. *J Coast Sci* 1:33–40
- Yasin MA, Sukiyah E, Isnaniawardhani V (2016) Grain size analysis of quaternary sediments from Kendari Basin, Indonesia. *Int J Sci Res* 5:1748–1751
- Yu SY, Colman SM, Li L (2016) BEMMA: A Hierarchical Bayesian End-Member Modeling Analysis of Sediment Grain-Size Distributions. *Math Geosci* 48:723–741. <https://doi.org/10.1007/s11004-015-9611-0>
- Zhang, W, Zheng J, Ji X, et al (2013) Surficial Sediment Distribution And The Associated Net Sediment Transport Pattern In The Pearl River Estuary, South China. *Cont Shelf Res* 61–62:41–51



## **Funding**

The authors declare that no funds, grants, or other support were received during the preparation of this manuscript.

## **Declaration Of Competing Interest**

The authors declare that they have no known competing financial interests or personal relationships that could have appeared to influence the work reported in this paper.

## **Author Contributions**

All authors contributed to the study's conception and design. Material preparation, data collection and analysis were performed by Lynda-Uta Edet Okon, Jaya Kumar Seelam, Suneeta Kumari and Lavanya Hemanath. Lynda-Uta Edet Okon wrote the first draft of the manuscript and all authors commented on previous versions. All authors read and approved the final manuscript.

## **Data Availability**

The datasets generated during and analysed during the current study are available from the corresponding author upon reasonable request.

## **Acknowledgments**

The authors acknowledge the support and facilities provided by the Director, CSIR-National Institute of Oceanography. The first author acknowledges The World Academy of Sciences (TWAS) and the Council of Scientific & Industrial Research, New Delhi (CSIR). The help rendered by the staff of the Ocean Engineering Division, CSIR-NIO, is placed on record for their assistance in sediment collection and sieve analysis. We also thank the editor and the reviewers for their constructive and meticulous reviews that have helped improve this manuscript's quality. This is NIO contribution no: \_\_\_\_\_ (will be filled after acceptance of manuscript). This article forms a part of the PhD thesis of the first author, registered at Bharathidasan University, Tiruchirappalli, India.